Available online at www.sciencedirect.com

ScienceDirect

Catalysis Today 131 (2008) 553–558

CATALYSIS TODAY

www.elsevier.com/locate/cattod

Performance of Pd catalysts supported on nanocrystalline α-Al_2O_3 and Ni-modified α-Al_2O_3 in selective hydrogenation of acetylene

Nitikon Wongwaranon [a], Okorn Mekasuwandumrong [b],
Piyasan Praserthdam [a], Joongjai Panpranot [a,*]

[a] *Center of Excellence on Catalysis and Catalytic Reaction Engineering, Department of Chemical Engineering, Faculty of Engineering, Chulalongkorn University, Bangkok 10330, Thailand*

[b] *Department of Chemical Engineering, Faculty of Engineering and Industrial Technology, Silpakorn University, Nakhonpathom, Thailand*

Available online 26 November 2007

Abstract

Nanocrystalline α-Al_2O_3 and Ni-modified α-Al_2O_3 have been prepared by sol–gel and solvothermal methods and employed as supports for Pd catalysts. Regardless of the preparation method used, $NiAl_2O_4$ spinel was formed on the Ni-modified α-Al_2O_3 after calcination at 1150 °C. However, an addition of NiO peaks was also observed by X-ray diffraction for the solvothermal-made Ni-modified α-Al_2O_3 powder. Catalytic performances of the Pd catalysts supported on these nanocrystalline α-Al_2O_3 and Ni-modified α-Al_2O_3 in selective hydrogenation of acetylene were found to be superior to those of the commercial α-Al_2O_3 supported one. Ethylene selectivities were improved in the order: Pd/Ni-modified α-Al_2O_3–sol–gel > Pd/Ni-modified α-Al_2O_3-solvothermal ≈ Pd/α-Al_2O_3–sol–gel > Pd/α-Al_2O_3-solvothermal ≫ Pd/α-Al_2O_3-commerical. As revealed by NH_3 temperature program desorption studies, incorporation of Ni atoms in α-Al_2O_3 resulted in a significant decrease of acid sites on the alumina supports. Moreover, XPS revealed a shift of Pd 3d binding energy for Pd catalyst supported on Ni-modified α-Al_2O_3–sol–gel where only $NiAl_2O_4$ was formed, suggesting that the electronic properties of Pd may be modified.

Keywords: Nanocrystalline α-Al_2O_3; Ni-modified α-Al_2O_3; Solvothermal; Sol–gel; Selective acetylene hydrogenation; Nickel aluminate

1. Introduction

The selective hydrogenation of acetylene in ethylene rich stream is a crucial process in polyethylene production since acetylene poisons the polymerization catalysts [1,2]. Pd-based catalyst supported on alumina with low Pd loading (0.1–0.3 wt.%) is typically employed for this reaction due to its good activity and selectivity and the easily desorption of ethylene on the catalyst surface. With respect to selectivity changes, catalysts of low Pd dispersion have been suggested to give better selectivity towards ethylene at high acetylene conversions [3–5]. The alumina used as Pd catalyst support in this reaction contains mostly the alpha phase alumina since it possesses relatively low specific surface area and low acidity compared to other 'transition' alumina. Recent reports have shown development of new efficient catalysts for the selective hydrogenation of acetylene including the glow discharge plasma-prepared Pd/α-Al_2O_3 [6], Pd on nano-sized TiO_2 [7,8], and zeolite-supported Pd-Ag catalysts [9].

In recent years, nanocrystalline materials have gained considerable interest in the field of catalysis because they show significant differences in terms of catalytic activity and selectivity compared with those synthesized in micron scale. For examples, Co catalysts supported on nanocrystalline Al_2O_3 [10] and ZrO_2 [11] have been found to exhibit higher hydrogenation activities and selectivities toward long chain hydrocarbons than those of the commercial micron-sized Al_2O_3 and ZrO_2 supported ones. Physical and chemical properties of TiO_2 are modified when they are synthesized in the nanometer range resulting in an improvement of its photocatalytic activity [12].

Several techniques have been reported for preparation of nanocrystalline 'transition' alumina such as sol–gel method [13], hydrothermal synthesis [14], microwave synthesis [15], emulsion evaporation [16,17], precipitation from solution [18],

---

* Corresponding author. Tel.: +66 2 2186869; fax: +66 2 2186877.
E-mail address: joongjai.p@eng.chula.ac.th (J. Panpranot).

0920-5861/$ – see front matter © 2007 Elsevier B.V. All rights reserved.
doi:10.1016/j.cattod.2007.10.036

and solvothermal synthesis [19,20]. The sol–gel method is widely used due to its simplicity, however, the precipitated powders obtained are amorphous in nature and further heat treatment is required for crystallization. Solvothermal method is an alternative route for one-step synthesis of nanocrystalline material. Desired shape and size of particles can be produced by controlling process conditions such as solute concentration, reaction temperature, reaction time, and the type of solvent [21].

In the present study, nanocrystalline α-Al_2O_3 and Ni-modified α-Al_2O_3 have been synthesized via sol–gel and solvothermal methods and employed as supports for Pd catalysts for selective hydrogenation of acetylene. Modification of nanocrystalline α-Al_2O_3 with nickel is also interesting because it can form nickel aluminate spinel ($NiAl_2O_4$) which is a highly stable material that can have beneficial effect on the catalyst performance. Moreover, formation of $NiAl_2O_4$ in some Ni-based hydrogenation catalysts has shown high resistance to coke formation [22–24].

2. Experimental

2.1. Preparation of Nanocrystalline α-Al_2O_3 and Ni-modified α-Al_2O_3

Nanocrystalline α-Al_2O_3 and Ni-modified α-Al_2O_3 were prepared by sol–gel and solvothermal methods. For the sol–gel method, 24 g of aluminium nitrate nonahydrate (Aldrich) was dissolved in 50 cc of ethanol. The experiment was conducted in the reflux-condenser reactor at the temperature about 70–80 °C for 18 h. Then, urea solution, which consist of 60 g of urea and 50 ml of distilled water, was added to adjust pH of sol. The mixture was rested at the same temperature for 24 h to be gelled at neutral condition. The obtained product was calcined with 2 steps heating rate to avoid overflowing of gel during calcinations, i.e. 3 °C/min from room temperature to 500 °C and continue heating at 5 °C/min to 1150 °C. Then, temperature was hold for 3 h. For the preparation of Ni-modified α-Al_2O_3, a desired amount of nickel nitrate-6-hydrate (Aldrich) was added to the precursor mixture and then followed the same procedures as that of α-Al_2O_3.

For the solvothermal method, α-Al_2O_3 and Ni-modified α-Al_2O_3 were prepared using a mixture of aluminum isopropoxide 15.0 g and appropriate amount of nickel(II) acetylacetonate. The starting materials were suspended in 100 mL of toluene in beaker, and then set up in autoclave. In the gap between the beaker and autoclave wall, 40 mL of toluene was added. After the autoclave was completely, the suspension was heated to 300 °C at the rate of 2.5 °C/min and held at that temperature for 2 h. However, the same synthesis method is performed at various holding temperature. Autogenous pressure during the reaction gradually increased as temperature was raised. Then the autoclave was cooled to room temperature. After the autoclave was cooled, the resulting products were washed repeatedly with methanol by centrifugation and dried in air. The calcination of the obtained product carried out in a furnace. The product was heated at a rate of 10 °C/min to a desired temperature 1150 °C and held at that temperature for 1 h. For comparison purposes, a commercial α-Al_2O_3 (JRC-ALO2) was also employed as Pd catalyst support.

2.2. Preparation of α-Al_2O_3 supported Pd catalysts

The Pd/α-Al_2O_3 catalysts were prepared by incipient wetness impregnation of Al_2O_3 support with a desired amount of an aqueous solution of palladium(II) nitrate hydrate (Aldrich). The catalysts were dried overnight at 110 °C and then calcined in N_2 flow 60 cm^3/min with a heating rate of 10 °C/min until the temperature reached 500 °C and then in air flow 100 cm^3/min at 500 °C for 2 h. The final Pd loading of the catalysts was determined by atomic absorption spectroscopy (Varian Spectra A800) to be ca. 0.3 wt.%.

2.3. Catalyst Characterization

Surface area measurements were carried out by nitrogen adsorption in a Micromeritic Chemisorb 2750 system. Each sample was degassed at 200 °C for 2 h. The analysis gas consisting of 30% N_2 in helium was adsorbed on the samples at low temperature by dipping cell into liquid nitrogen dewar. X-ray diffraction patterns of the catalyst samples were obtained with a SIEMENS D5000 X-ray diffractometer using Cu Kα radiation with a Ni filter. The pattern were recorded between 20° and 80° (2θ) using a scanning velocity of 0.02°/s. Metal active sites were measured using CO chemisorption technique at room temperature in a Micromeritic Chemisorb 2750 automated system attached with ChemiSoft TPx software. Before chemisorption measurement, the sample was reduced in a H_2 flow at 150 °C for 2 h then cooled down to ambient temperature in a He flow. Ammonia temperature program desorption (NH_3-TPD) was also performed in a Micromeritic Chemisorb 2750 automated system attached with ChemiSoft TPx software. Approximately 100 mg of catalyst was placed in a quartz tube in a temperature-controlled oven. The samples adsorbed ammonia at 40 °C, then heated up to 650 °C at a heating rate of 10 °C/min. The distribution of palladium on catalyst supports were observed using AJEM-200CX transmission electron microscope operated at 160 kV. Surface compositions of the catalysts were analyzed using an AMICUS photoelectron spectrometer equipped with Mg Kα X-ray as primary excitation and KRATOS VISION2 software. XPS elemental spectra were acquired with 0.1 eV energy step at a pass energy of 75 kV. The C 1s line was taken as an internal standard at 285.0 eV.

2.4. Reaction study

Catalytic performance of the catalysts was studied in selective hydrogenation of acetylene. The experiment was performed in a quartz tube reactor (i.d. 10.1 mm). Before starting of the reaction, the catalyst was reduced in H_2 at 150 °C for 2 h. Then the reactor was purged with argon and cooled down to the reaction temperature, 40 °C. Feed gas composed of 1.5% C_2H_2, 1.7% H_2, and balanced C_2H_4 (TIG Co., Ltd.), a GHSV of 39435, 24433, 16901 and 9288 h^{-1} were used. The composition of product and feed stream were analyzed by a Shimadzu GC 8A equipped with TCD and FID detectors (molecular sieve-5A and carbosieve S2 columns, respectively). Acetylene conversion as used herein is defined as moles of acetylene converted with respect to acetylene in feed. Ethylene selectivity is defined as the percentage of acetylene hydrogenated to ethylene over totally hydrogenated acetylene. The ethylene being hydrogenated to ethane (ethylene loss) is the difference between all the hydrogen consumed and all the acetylene which has been totally hydrogenated.

3. Results and discussion

3.1. Catalyst characterization

The XRD patterns of the sol–gel- and the solvothermal-made Pd/α-Al_2O_3 and the Pd/Ni-modified α-Al_2O_3 catalysts with Ni/Al atomic ratio 0.5 after calcinations at 1150 °C are shown in Fig. 1. The patterns in the lower half of the figure correspond to the sol–gel-made powder while the patterns in the upper part of the figure are for those prepared by solvothermal synthesis. Both the sol–gel- and solvothermal-made Pd/α-Al_2O_3 catalysts exhibited all the characteristic peaks of α-Al_2O_3 structure. While the diffraction lines for Pd/Ni-modified α-Al_2O_3 catalyst could be assigned to a spinel-type $NiAl_2O_4$ structure; space group Fd3m [25]. Additional peaks corresponding to NiO were also presented at 43.3 and 62.9° 2θ for the product obtained from solvothermal synthesis. The XRD characteristic peaks associated with Pd^0 or PdO phase were not observed in all the samples. This was probably due to the very low amount of Pd present and/or a very good dispersion of Pd phase on all the alumina supports.

TEM micrographs were taken in order to physically measure the size of the palladium oxide particles and/or palladium clusters. It can be seen that the sol–gel made catalyst (Fig. 2a and b) was consisted of agglomerated particles with primarily irregular shape structure. For those prepared by solvothermal method, agglomeration of finger-like particles were observed for the Pd/α-Al_2O_3 whereas spherical-shape particles were found for the Pd/Ni-modified α-Al_2O_3 catalysts (Fig. 2c and d, respectively). The finger-like α-Al_2O_3 particles are normally obtained by calcination of the solvothermal-made α-Al_2O_3 powders at high temperature [26,27]. Based on TEM analysis, palladium particles/clusters with average particle size ca. 5–10 nm were found to be deposited on the alumina supports.

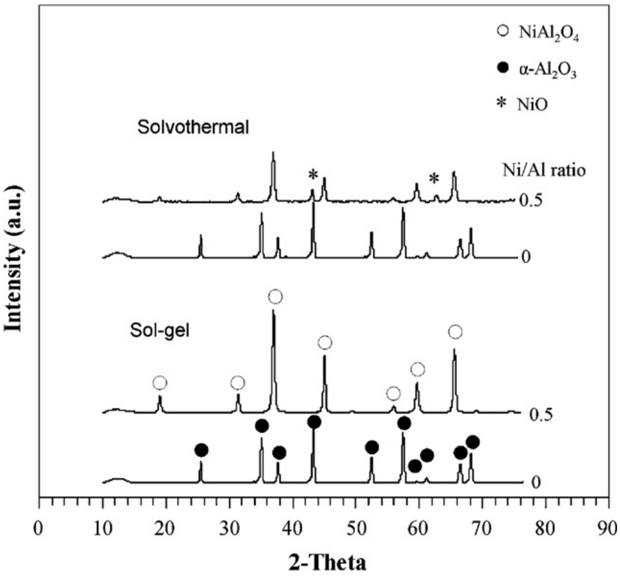

Fig. 1. XRD patterns of the various Pd catalysts supported on nanocrystalline α-Al_2O_3 and Ni-modified α-Al_2O_3 prepared by sol–gel and solvothermal methods.

The physical and chemical properties of Pd/α-Al_2O_3 and Pd/Ni-modified α-Al_2O_3 catalysts are summarized in Table 1. The average crystallite size of each crystal phase was calculated from the Scherrer equation. The average crystallite sizes of the α-Al_2O_3 prepared by sol–gel and solvothermal method were 34 and 58 nm, respectively. While, the crystallite sizes of $NiAl_2O_4$ formed in the Ni-modified α-Al_2O_3 prepared by sol–gel and solvothermal method were 23 and 27 nm, respectively. In all cases, the average crystallite sizes of $NiAl_2O_4$ were smaller than those of α-Al_2O_3. Such results suggest that crystal growth rate for $NiAl_2O_4$ was slower than that of α-Al_2O_3. The surface areas of all the catalysts were not significantly different and still quite low, due probably to high agglomeration of these nanocrystalline particles during calcinations at high temperature. The amounts of CO chemisorption on the catalysts, the Pd dispersions, and the average Pd metal particle sizes determined from CO chemisorption are also given in Table 1. The pulse CO chemisorption technique was based on the assumption that one carbon monoxide molecule adsorbs on one palladium site [28–32]. The amounts of CO chemisorption decreased from 7.5 to 5.4×10^{17} and 8.1 to 7.4×10^{17} sites/g cat. corresponding to the decreasing in Pd metal dispersion from 4.4 to 3.2 and 4.8 to 4.3% by modification with Ni atoms by sol–gel and solvothermal method, respectively. The percentages of Pd dispersion calculated from the CO chemisorption results were in the order Pd/α-Al_2O_3-solvothermal > Pd/α-Al_2O_3–sol–gel ≈ Pd/Ni-modified α-Al_2O_3-solvothermal > Pd/Ni-modified α-Al_2O_3–sol–gel. The average Pd^0 particle sizes for all the catalysts were calculated to be 24–35 nm.

Fig. 3 shows the NH_3 temperature program desorption profiles for the sol–gel and solvothermal-made α-Al_2O_3 and the Ni-modified α-Al_2O_3 supports. Comparing the desorption peak area of the reference γ-alumina, the desorption peak areas of the nanocrystalline α-Al_2O_3 powders obtained from both sol–gel and solvothermal syntheses were relatively low due probably to the dramatically decrease of the surface area after calcination at high temperature. However, two desorption peaks corresponding to different acid sites were still observed at ca. 320 and 400–500 °C for both α-Al_2O_3 samples. For the Ni-modified α-Al_2O_3–sol–gel, no distinctive peaks were observed and the profiles became almost flat. Such results indicate that acidity of the α-Al_2O_3 samples was drastically decreased by incorporation of Ni atoms. The results are in good agreement with those reported by other researchers. For examples, Otero Areán et al. [33] measured acidity of Ni-doped alumina by IR spectroscopy of CO adsorbed at liquid nitrogen temperature. A

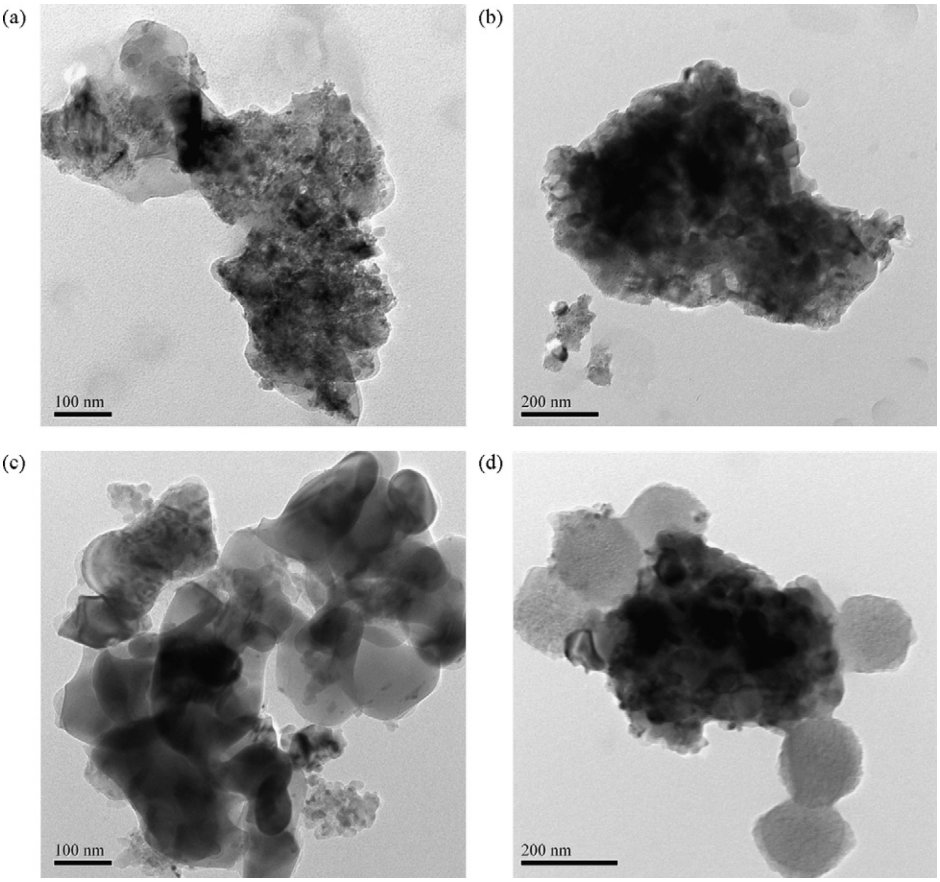

Fig. 2. TEM micrographs of (a) Pd/α-Al_2O_3–sol–gel, (b) Pd/Ni-modified α-Al_2O_3–sol–gel, (c) Pd/α-Al_2O_3-solvothermal, and (d) Pd/Ni-modified α-Al_2O_3-solvothermal.

decrease in both Lewis and Brønsted acidity was observed as the Ni contents increased in the Ni-alumina solid solution. The very low Brønsted acidity also appears to be typical for many oxide spinels as well as other aluminate spinels such as $MgAl_2O_4$ and $ZnAl_2O_4$ [34,35]. A small broad peak was observed for the Ni-modified α-Al_2O_3-solvothermal due probably to the formation of NiO species in which some acidity may be remained.

Because of its surface sensitivity, XPS is used to monitor the interaction between surface Pd and the alumina supports. The elemental scans for Pd 3d of the Pd/α-Al_2O_3 and the Pd/Ni-modified α-Al_2O_3 catalysts are shown in Fig. 4. It was found that the binding energy of Pd 3d for the Pd catalyst supported Ni-modified α-Al_2O_3 prepared by sol–gel shifted to lower binding energy while for those of all the other catalysts, the binding energies for Pd 3d were at the same binding energies. It

Table 1
Characteristics of the various Pd/α-Al_2O_3 and Pd/Ni-modified α-Al_2O_3 catalysts

Sample	d_{XRD}[a] (nm)	BET surface area (m^2/g)	CO chemisorption ($\times10^{17}$ sites/g cat.)	% Dispersion	d_P[b] Pd^0 (nm)
Sol–gel					
Pd/α-Al_2O_3	34[c]	1.5	7.51	4.42	25
Pd/Ni-α-Al_2O_3	27[d]	1.9	5.37	3.16	35
Solvothermal					
Pd/α-Al_2O_3	54[c]	4.7	8.10	4.76	24
Pd/Ni-α-Al_2O_3	23[d], 26[e]	1.4	7.35	4.32	26
Commercial					
Pd/α-Al_2O_3	391.6[c]	0.5	5.91	3.48	32

[a] Average crystallite size calculated by Scherrer equation.
[b] Average Pd metal particle size calculated from CO chemisorption results. $d_P = 1.12/D$ where D = Pd dispersion [25].
[c] α-Al_2O_3.
[d] $NiAl_2O_4$.
[e] NiO.

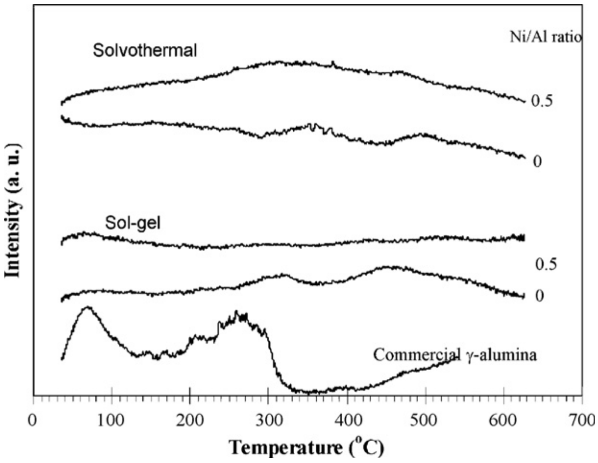

Fig. 3. NH_3 temperature program desorption profiles for the sol–gel and solvothermal-made α-Al_2O_3 and the Ni-modified α-Al_2O_3 supports.

is likely that Pd catalyst supported on $NiAl_2O_4$ spinel may result in a lower interaction between Pd and the alumina support.

3.2. Catalyst performance in selective acetylene hydrogenation

The catalyst performance in selective hydrogenation of acetylene to ethylene was studied for all the catalyst samples using a fixed bed flow reactor. Changes in ethylene selectivity with acetylene conversion for Pd/α-Al_2O_3 and Pd/Ni-modified α-Al_2O_3 catalysts are shown in Fig. 5. In general, ethylene selectivity decreases with increasing acetylene conversion due to the fact that the ethylene is produced as an intermediate in acetylene hydrogenation reaction. Compared to Pd catalyst supported on the commercial α-Al_2O_3, the ones supported on nanocrystalline α-Al_2O_3 and Ni-modified α-Al_2O_3 showed superior catalytic performances in selective acetylene hydrogenation with Pd/Ni-modified α-Al_2O_3 exhibited higher selectivity than Pd/α-Al_2O_3. When comparing the samples prepared by different techniques, the sol–gel-made samples showed higher ethylene selectivity than those of the solvothermal-derived ones. The ethylene selectivity was improved in the order: Pd/Ni-modified α-Al_2O_3-sol–gel > Pd/Ni-modified α-Al_2O_3-solvothermal ≈ Pd/α-Al_2O_3–sol–gel > Pd/α-Al_2O_3-solvothermal ≫ Pd/α-Al_2O_3-commercial.

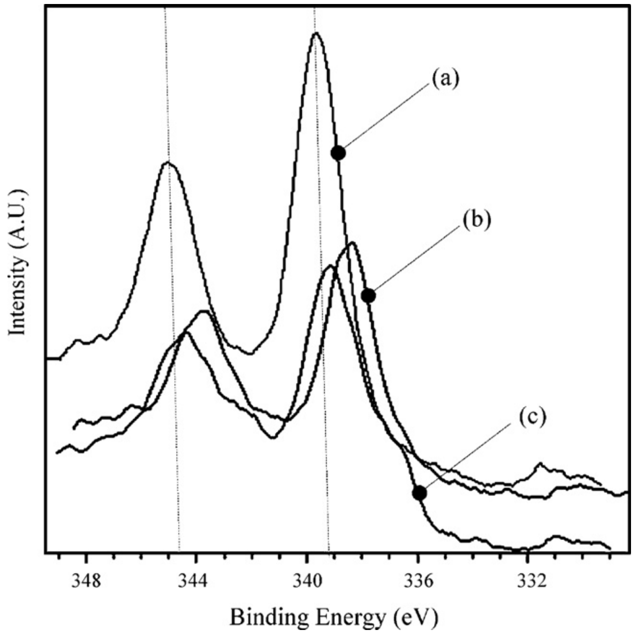

Fig. 4. XPS results of Pd 3d for (a) Pd/α-Al_2O_3–sol–gel, (b) Pd/Ni-modified α-Al_2O_3–sol–gel and (c) Pd/Ni-modified α-Al_2O_3-solvothermal.

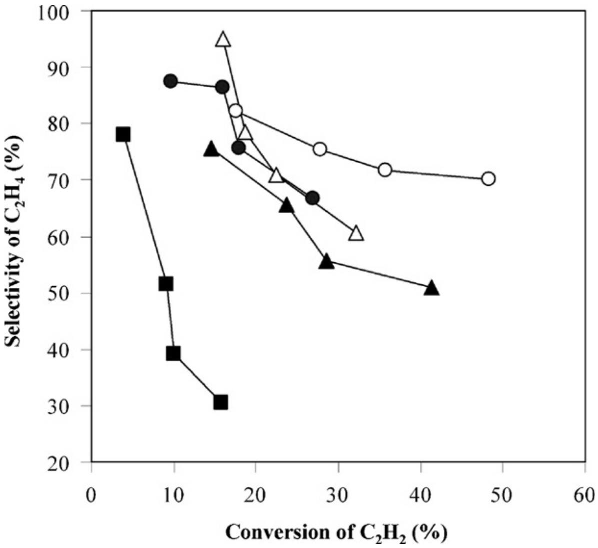

Fig. 5. Performance of sol–gel (circle; ○) and solvothermal (triangle; △) made Pd/α-Al_2O_3 (filled symbols), Pd/commercial α-Al_2O_3 (filled square; ■) and Pd/Ni-modified α-Al_2O_3 (open symbols) catalysts in selective acetylene hydrogenation.

During long-time investigation by many research groups, the catalytic activity and ethylene selectivity in the selective acetylene hydrogenation in excess ethylene over Pd-based catalysts are found to be dependent on many factors such as metal dispersion (Pd metal particle size) [7], thermodynamic adsorption differences between acetylene and ethylene [36], and carbonaceous product formation [37,38], etc. Based on the reaction mechanisms for acetylene hydrogenation on Pd/Al_2O_3 catalysts in the literatures [39], there are three active sites on the Pd metal surface and one active site on the alumina support. The three sites on the palladium surface are responsible for selective hydrogenation of acetylene to ethylene, direct ethane formation from acetylene and oligomer formation whereas ethylene hydrogenation is believed to take place on the support by means of a hydrogen transfer mechanism. It was claimed that the carbonaceous deposits present act as bridges for hydrogen spillover [40]. It is well known that acidity on alumina surface promotes formation of carbonaceous deposits on catalyst surface. When Ni was incorporated in alumina lattice (i.e., in terms of $NiAl_2O_4$ formation), the acidity of alumina decreased drastically and thus reduced the formation of carbonaceous deposits and hydrogen spillover. In summary, Pd catalyst supported on Ni-modified α-Al_2O_3 can be used as an effective catalyst for producing high ethylene selectivities at relatively high acetylene conversions especially when $NiAl_2O_4$ are formed. Promotion with other second metals such as Ag is then not necessary in order to improve the catalytic performance of these Pd-based catalysts.

4. Conclusions

The catalytic performance of Pd catalysts supported on nanocrystalline α-Al_2O_3 and Ni-modified α-Al_2O_3 prepared by sol–gel and solvothermal methods was studied in the selective hydrogenation of acetylene in excess ethylene. While the use of sol–gel method resulted in only $NiAl_2O_4$ formation, those prepared by solvothermal gave both $NiAl_2O_4$ and NiO species. Acidity of the nanocrystalline α-Al_2O_3 was significantly decreased by incorporation of Ni atoms in α-Al_2O_3. Ethylene selectivities were improved in the order: Pd/Ni-modified α-Al_2O_3–sol–gel $>$ Pd/Ni-modified α-Al_2O_3-solvothermal $\approx$ Pd/α-Al_2O_3–sol–gel $>$ Pd/α-Al_2O_3-solvothermal $\gg$ Pd/α-Al_2O_3-commercial. The improvement in catalyst performance is probably due to both a decrease in surface acidity of α-Al_2O_3 and modification of Pd surface activity due to $NiAl_2O_4$ formation.

Acknowledgements

Financial supports from the Thailand Research Fund (TRF), the Research and Development Institute of Silpakorn University, and the Graduate School of Chulalongkorn University are gratefully acknowledged.

References

[1] Y.-J.Huang, C.F. Shun, L.G. Daniel, E.L. Mohundro, J.E. Hartgerink, US Patent 5,332,705 (1994).
[2] Q. Zhang, J. Li, X. Liu, Q. Zhu, Appl. Catal. A 197 (2000) 221.
[3] S. Hub, L. Hilaire, R. Touroude, Appl. Catal. 36 (1988) 307.
[4] J.P. Boitiaux, J. Cosyns, S. Vasudevan, Appl. Catal. 6 (1983) 41.
[5] Á. Sárkány, A.H. Weiss, L. Guczi, J. Catal. 98 (1986) 550.
[6] M.H. Chen, W. Chu, X.Y. Dai, X.W. Zhang, Catal. Today 89 (2004) 201.
[7] J. Panpranot, K. Kontapakdee, P. Praserthdam, Appl. Catal. A 314 (2006) 128.
[8] J. Hong, W. Chu, M. Chen, X. Wang, T. Zhang, Catal. Commun. 8 (2007) 593.
[9] W. Huang, J.R. McCormick, R.F. Lobo, J.G. Chen, J. Catal. 246 (2007) 40.
[10] K. Pansanga, O. Mekasuwandumrong, J. Panpranot, P. Praserthdam, Korean J. Chem. Eng. 24 (2007) 397.
[11] J. Panpranot, N. Taochaiyaphoom, P. Praserthdam, Mater. Chem. Phys. 94 (2005) 207.
[12] U. Diebold, Surf. Sci. Rep. 48 (2003) 53.
[13] C.J. Brinker, G.W. Scherrer, Sol–Gel Science: The Physics and Chemistry of Sol–Gel Processing, Academic Press, San Diego, 1990.
[14] W.H. Dawson, Am. Ceram. Soc. Bull. 67 (1988) 1673.
[15] S.G. Deng, Y.S. Lin, J. Mater. Sci. Lett. 16 (1997) 1291.
[16] Y. Sarikaya, I. Sevinc, M. Akinc, Powder Technol. 116 (2001) 109.
[17] I. Sevinc, Y. Sarikaya, M. Akinc, Ceram. Int. 1 (1991) 17.
[18] W.B. Scott, E. Matijevic, J. Colloid Interface Sci. 66 (1978) 447.
[19] M. Inoue, H. Kominami, T. Inui, J. Am. Ceram. Soc. 73 (1990) 1100.
[20] M. Inoue, H. Kominami, T. Inui, J. Am. Ceram. Soc. 75 (1996) 2597.
[21] Y. Deng, X. Zhou, G. Wei, J. Liu, C.W. Nan, S. Zhao, J. Phys. Chem. Solids 63 (2002) 2119.
[22] A. Al-Ubaid, E.E. Wolf, Appl. Catal. 40 (1998) 73.
[23] A. Bhattacharyya, V.W. Chang, Stud. Surf. Sci. Catal. 88 (1994) 207.
[24] J.A. Peña, J. Herguido, C. Guimon, A. Monzón, J. Santamaría, J. Catal. 159 (1996) 313.
[25] A.R. West, Solid State Chemistry and its Application, John Wiley & Sons, New York, 1997.
[26] O. Mekasuwandumrong, V. Pavarajarn, M. Inoue, P. Praserthdam, Mater. Chem. Phys. 100 (2006) 445.
[27] O. Mekasuwandumrong, P.L. Silveston, P. Praserthdam, M. Inoue, V. Pavarajarn, W. Tanakulrungsank, Inorg. Chem. Commun. 6 (2003) 930.
[28] N. Mahata, V. Vishwanathan, J. Catal. 196 (2000) 262.
[29] S.H. Ali, J.G. Goodwin Jr., J. Catal. 176 (1998) 3.
[30] E.A. Sales, G. Bugli, A. Ensuque, M.J. Mendes, F. Bozon-Verduraz, Phys. Chem. Chem. Phys. 1 (1999) 491.
[31] A. Sarkany, Z. Zsoldos, B. Furlong, J.W. Hightower, L. Guczi, J. Catal. 141 (1993) 566.
[32] N.K. Nag, Catal. Lett. 24 (1994) 37.
[33] C. Otero Arean, M. Penarroya Mentruit, A.J. Lopez Lopez, J.B. Parra, Colloids Surf. A 180 (2001) 253.
[34] C. Otero Arean, C. Mas Carbonell, Vib. Spectrofc. 8 (1995) 411.
[35] C. Otero Arean, B. Sintes Sintes, G. Turnes Palomino, C. Mas Carbonell, E. Escalona Platero, J.B. Parra Soto, Microporous Mater. 8 (1997) 187.
[36] G.C. Bond, Catalysis by Metals, Academic Press, London, 1962.
[37] A. Borodzinski, A. Cybulski, Langmuir 13 (1997) 883.
[38] A. Borodzinski, A. Cybulski, Appl. Catal. A 198 (2000) 51.
[39] R.N. Lamb, B. Ngamsom, D.L. Trimm, B. Gong, P.L. Silveston, P. Praserthdam, Appl. Catal. A 268 (2004) 43.
[40] S. Asplund, J. Catal. 158 (1996) 267.